Research Article

Ecological vulnerability assessment and driving force analysis of small watersheds in Hilly Regions using sensitivity-resilience-pressure modeling

Jing-tao Shi[1], Ge Gao[1], Jun-jian Liu[1*], Yu-ge Jiang[1], Bo Li[1], Xiao-yan Hao[2], Jun-chao Zhang[3], Zhao-yi Li[4], Huan Sun[1]

[1] *Langfang Natural Resources Comprehensive Survey Center, China Geological Survey, Langfang 065000, Hebei Province, China.*
[2] *Pingquan City Department of Natural Resources and Planning, Pingquan 067500, Hebei Province, China.*
[3] *Pingquan soil and water Conservation Construction Service Center, Pingquan 067500, Hebei Province, China.*
[4] *Chinese Academy of Geological Sciences, Beijing 100037, China.*

Abstract: Pingquan City, the origin of five rivers, serves as the core water conservation zone for the Beijing-Tianjin-Hebei region and exemplifies the characteristics of small watersheds in hilly areas. In recent years, excessive mining and intensified human activities have severely disrupted the local ecosystem, creating an urgent need for ecological vulnerability assessment to enhance water conservation functions. This study employed the sensitivity-resilience-pressure model, integrating various data sources, including regional background, hydro-meteorological data, field investigations, remote sensing analysis, and socioeconomic data. The weights of the model indices were determined using an entropy weighting model that combines principal component analysis and the analytic hierarchy process. Using the ArcGIS platform, the spatial distribution and driving forces of ecological vulnerability in 2020 were analyzed, providing valuable insights for regional ecological restoration. The results indicated that the overall Ecological Vulnerability Index (EVI) was 0.389, signifying moderate ecological vulnerability, with significant variation between watersheds. The Daling River Basin had a high EVI, with ecological vulnerability primarily in levels IV and V, indicating high ecological pressure, whereas the Laoniu River Basin had a low EVI, reflecting minimal ecological pressure. Soil type was identified as the primary driving factor, followed by elevation, temperature, and soil erosion as secondary factors. It is recommended to focus on key regions and critical factors while conducting comprehensive monitoring and assessment to ensure the long-term success of ecological management efforts.

Keywords: Beijing-Tianjin-Hebei water conservation zone; Spatital analysis; SRP model; GIS; Watershed variation

Introduction

Against the backdrop of ongoing global environmental changes, the stability and sustainability of ecosystems have become focal points for the scientific community, policymakers, and the public (De et al. 2010; Cui, 2012), particularly in regions characterized by complex terrain and intense human activities. Ecological vulnerability assessment, which evaluates an ecosystem's ability to resist, recover from, and adapt to natural or human-induced pressures, has emerged as a key research direction in the fields of ecology (Fan et al. 2009; Li et al. 2006; Gao et al. 2018), environmental science, and geography. Its importance is increasingly recognized in the domain of ecological restoration (Zhang et al. 2018).

Research on ecological vulnerability in basins has gained significant momentum in recent years, Various methodologies and models, and more

recently, the integration of remote sensing and Geographic Information Systems (GIS), have been employed to assess and map ecological vulnerability (Lan et al. 2023). For example, Zou and Chang (2021) evaluated the ecological vulnerability of Jilin Province by determining index weights through a combination of subjective and objective methods, and they established the Sensitivity-Resilience-Pressure (SRP) model; Zhang et al. (2009) applied causal theory to assess the ecological vulnerability of the middle and lower reaches of the Hanjiang River Basin, classifying the system at the watershed scale. Leitao et al. (2002) greatly enhanced the efficiency and accuracy of ecological vulnerability assessments through the combined application of GIS and RS technologies, Wang and Su (2002) employed this approach to develop a "pressure-state-response" framework for Hanzhong City, and they objectively evaluated large-scale, complex environments, revealing patterns of spatial-temporal variations in environmental vulnerability.

Despite the advancements in this field, For example, Li et al. (2015) used the CLUS-S model to explore the response of landscape ecological risk to land use change in the Luanhe River Basin, there remains a notable gap in the understanding of ecological vulnerability in small watersheds located in hilly areas, particularly in regions like Pingquan City, which serves as the source of five major rivers and is pivotal for water conservation in the Beijing-Tianjin-Hebei region. The unique geographical and ecological features of these areas, coupled with intensifying anthropogenic pressures such as mining activities and land-use changes, have led to an imbalance in ecosystems, necessitating a comprehensive evaluation of their ecological vulnerability.

Currently, common methods for ecological vulnerability assessments include Principal Component Analysis (PCA) (Zou and Yoshino, 2017; Hou et al. 2015a), fuzzy mathematics (Ippolito et al. 2010; Jiang et al. 2009), grey evaluation (Zhang et al. 2017; Sahoo et al. 2016), the matter-element extension method (Xu et al. 2017; Shan et al. 2021), and the Analytic Hierarchy Process (AHP) (Hu et al. 2021; Hou et al. 2016b), PCA and AHP are widely used in environmental vulnerability assessments, as they enable analysis and decision-making based on hierarchical system results. In this study, we used the entropy model combining PCA and AHP to integrate regional background information, hydrometeorological data, field surveys, remote sensing analysis and socio-economic data (Wang et al. 2010), and was

committed to providing a detailed understanding of the spatial distribution and driving forces of ecological vulnerability, in order to provide support for the ecological restoration of the Beijing-Tianjin-Hebei water conservation functional area.

1 Study area

Pingquan City is located in the northeastern part of Hebei Province, at the junction of Liaoning Province, Inner Mongolia Autonomous Region, and Hebei Province. Five major rivers—namely, the Baohe River, Laoha River, Daling River, Laoniu River, and Qinglong River—originate here, all of which are headwaters with no external inflow. The region is situated at the convergence of three mountain ranges: The Yanshan, Qilaotu, and Nuruerhu mountains. The terrain is primarily composed of low and medium mountains and hills. The land slopes from high elevations in the north to lower elevations in the south and tilts from northwest towards the east. The mountain ranges are generally aligned in an east-west direction. The area's complex and varied topography, combined with numerous valleys and gullies, creates many microclimates. The average annual rainfall is approximately 540 mm, though there are significant interannual variations. The study area is located in the transitional zone between warm temperate deciduous broad-leaved forests and temperate mixed coniferous and broad-leaved forests, resulting in a complex and unique vegetation landscape.

Pingquan City lies on the border of the Yanshan platform fold of the North China Platform and the Inner Mongolia Axis, characterized by multiple tectonic complexes and overlays. The lithology of the study area is diverse and geologically continuous, with Mesozoic intrusive rocks in the western and northeastern parts, Precambrian intrusive rocks in the northwestern part, Neoproterozoic metamorphic rocks and Paleozoic carbonates in the western region, and Paleozoic and Mesozoic clastic rocks predominantly in the eastern and southern parts (Fig. 1) (Shi et al. 2024).

The Luanhe River Basin serves as the foremost ecological barrier for the Beijing-Tianjin-Hebei metropolitan area (Xu et al. 2013), As a primary tributary of the Luanhe River system, the study area plays a key role in safeguarding and managing the "faucet" of the region, making it a critical water conservation zone for the Beijing-Tianjin-Hebei area. However, irrational mining activities and unbalanced human interventions have damaged the ecological landscape. Extensive rock
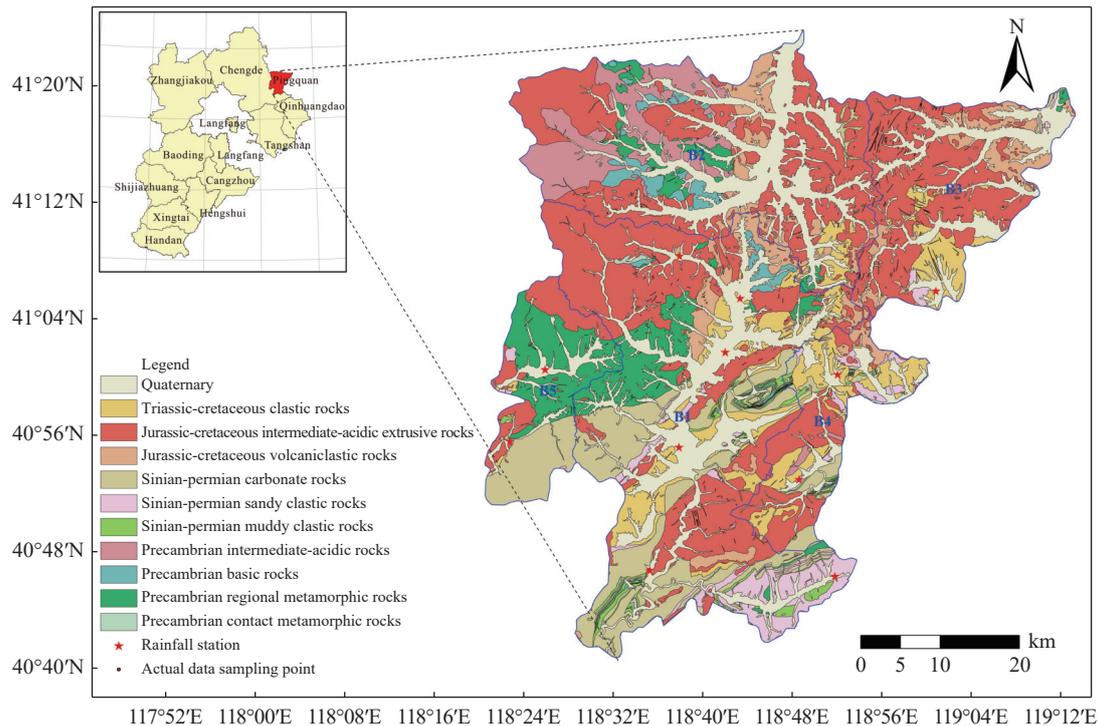
Fig. 1 Location and geologic map of the study area (B1: Cascade River Basin; B2: Laoha River Basin; B3: Daling River Basin; B4: Qinglong River Basin; B5: Laoniu River Basin)

outcrops, coupled with an ill-conceived industrial layout, have caused widespread water shortages, especially in some areas. Moreover, mining activities are concentrated in the upper reaches of the watersheds, leading to significant degradation of ecosystem integrity, imbalance in the temporal and spatial distribution of water resources, and escalating ecological vulnerability. Conducting an ecological vulnerability assessment of Pingquan City is essential to supporting the ecological restoration of the Beijing-Tianjin-Hebei water conservation zone.

2 Materials and methods

2.1 Establishment of the Evaluation Index System

Based on the SRP model (Wu et al. 2018), this study drew on the concept of ecosystem stability and systematically analyzed the combined effects of natural environmental factors, human disturbances, ecological sensitivity, and ecological adaptability on ecological vulnerability. The evaluation index system for assessing ecological vulnerability in Pingquan City was constructed by selecting three core factors: Ecosystem sensitivity, resilience, and pressure (Table 1). This framework was used to comprehensively assess the ecological vulnerability of the region.

2.2 Data collection and processing

The data used in this study primarily include regional background, meteorological data, topography, land use, field measurements, socio-economic and population data, and other relevant data for Pingquan City in 2020.

Regional background data encompass geological formations and soil types. The geological formation data were derived from 14 sheets of 1:50,000 scale basic geological maps from the National Geological Archives of China (https://www.ngac.org.cn). Soil type data were obtained from the National Earth System Science Data Center (https://www.geodata.cn).

Meteorological data consisted of annual precipitation, average annual temperature, and drought index. The annual precipitation data were collected from 12 basic rainfall stations in Pingquan City, representing the total monthly precipitation for 2020 (Fig. 1). These data were interpolated into a raster dataset using the ordinary Kriging method in ArcGIS. The average annual temperature data were sourced from the Earth Resources Data Cloud Platform (https://www.gis5g.com), while the drought index Idm was calculated using Equation (1):

$$I_{dm} = \frac{P}{T + 10} \tag{1}$$

Where: I_{dm} is the de Martonne aridity index, with

Table 1 Evaluation index system of SRP model for ecological vulnerability in Pingquan area

Target level	Factor layer	Indicator layer	Relationship type
Ecological vulnerability	Ecological sensitivity	Geo-construction (X1)	Proactively
		Elevation (X2)	Proactively
		Altitude (X3)	Proactively
		Annual rainfall (X4)	Pessimistic
		Average annual temperature (X5)	Pessimistic
		Dryness index (X6)	Pessimistic
		Vegetation cover (X7)	Pessimistic
		Soil erosion factor (X8)	Proactively
		Landscape fragmentation (X9)	Proactively
	Ecological resilience	Vegetation NPP (X10)	Pessimistic
		Soil type (X11)	Proactively
		Soil nutrient synthesis (X12)	Pessimistic
		Ecological richness (X13)	Pessimistic
	Ecological pressure	Population density (X14)	Proactively
		GDP (X15)	Proactively
		Food crop production (X16)	Proactively
		Gross output value of agriculture, forestry, livestock and fisheries (X17)	Proactively

lower values indicating more arid conditions; P is the average precipitation (mm); and T is the average temperature (°C).

Topography and land use data include elevation, slope, landscape fragmentation, and ecological abundance. Elevation data were obtained from a 90 m-resolution digital elevation model provided by the Geospatial Data Cloud (https://www.gscloud.cn/) and were used to extract elevation and slope information in ArcGIS. Landscape fragmentation was calculated using Equation (2) based on the third national land survey data for Chengde City (Qiu et al. 2007), utilizing the Perimeter-Area Ratio (PARA) as an indicator (Li and Huang, 2015). Ecological abundance data were determined in the following steps: first, forest land, water bodies, cropland, urban land, and bare land were extracted from RS images, and the area of each type of land use was derived at the county administrative scale; then, the ecological abundance index was calculated according to the Technical Criterion for Ecosystem Status Evaluation (HJ/192-2015):

$$PARA_j = \frac{TP_j}{TA_j} \qquad (2)$$

Where: $PARA_j$ is the perimeter-area ratio for land use type j; TP_j is the total perimeter of land use type j; and TA_j is the total area of land use type j. There is a positive correlation between $PARA$ values and landscape fragmentation.

Field measurement data include soil particle size, organic matter, N, P, and K (Fig. 1), Weathered crust profiles, gully valleys and agricultural fields were selected as sample sampling sites, which were used to calculate the soil erosion factor and comprehensive soil nutrient data. The soil erosion factor was calculated using the measured data on soil particle size and organic matter following the Technical Specification for Investigation and Assessment of National Ecological Status—Ecosystem Services Assessment (HJ/1173-2021) (Equation 3). Comprehensive soil nutrient data were evaluated based on soil N, P, and K data, and the comprehensive nutrient index was calculated using Equation (4) based on the classification of nutrient levels for each of these elements:

$$K_{EPIC} = \{0.2 + 0.3exp[-0.0256m_s(1 - m_{silt}/100)]\} \times$$
$$[m_{silt}/(m_c + m_{silt})]^{0.3} \times \{1 - 0.25orgC/[orgC +$$
$$exp(3.72 - 2.95orgC)]\} \times \{1 - 0.7(1 - m_s/100) +$$
$$exp[-5.51 + 22.9(1 - m_s/100)]\}$$
$$K = (-0.01383 + 0.51575K_{EPIC}) \times 0.1317 \qquad (3)$$

$$C_{cn} = \sum_{i=0}^{n} K_i f_i \cdots\cdots (i = 1, 2, 3, \cdots\cdots n) \qquad (4)$$

Where: K_{EPIC} is the soil erodibility factor calculated using the Eerosion-Productivity Impact Calculator (EPIC) model, expressed in (t·hm²·h)/(hm²·MJ·mm); m_s is the percentage of sand content (0.05−2 mm); m_{shit} is the percentage of silt content

(0.002–0.05 mm); m_c is the percentage of clay content (< 0.002 mm); org_C is the percentage of organic carbon content; K is the soil erodibility factor, expressed in $(t·hm^2·h)/(hm^2·MJ·mm)$; C_{cn} represents the contents of N, P, and K in the soil, respectively (Table 2); and f_i are the weighting factors for N, P, and K, which are 0.4, 0.4, and 0.2, respectively.

Socio-economic and population data were composed of population density, Gross Domestic Product (GDP), food crop production, and total output value of agriculture, forestry, animal husbandry, and fishery, all sourced from the 2020 Pingquan City Statistical Yearbook. These data were processed and aggregated at the county level and converted into raster datasets using ArcGIS.

Other data included vegetation coverage and net primary productivity of vegetation. Vegetation coverage was obtained from the MODIS index product, specifically using the May 2020 composite vegetation index (MOD13A13) at a resolution of 1 km. The maximum value composite method was applied to derive the normalized difference vegetation index values. NPP data were sourced from MOD17A3H, which has a resolution of 500 m.

2.3 Research methodology

2.3.1 Index normalization

Based on the relationship between ecological vulnerability and evaluation factors, ecological vulnerability indices were categorized into positive and negative indices. As ecological vulnerability increases, positively correlated indices increase, while negatively correlated indices decrease. It is assumed that the raw data for each ecological indicator, after normalisation, can be compared linearly on a scale from 0 to 1, i.e. the extent to which each indicator affects ecological vulnerability can be quantified and compared with each other. Consequently, In this study, the maximum-minimum normalization method was used to normalize the indices. This method reduced the influence of differences in scale among the indices, the selected maximum and minimum values are representative of the data range and distribution characteristics of the ecological indicator, thus

ensuring the accuracy and validity of the normalisation results, ensuring that the normalized values fell between 0 and 1. Positive and negative indices were normalized using Equations (5) and (6), respectively:

$$x = \frac{x_i - x_{imin}}{x_{imax} - x_{imin}} \tag{5}$$

$$x = \frac{x_{imax} - x_i}{x_{imax} - x_{imin}} \tag{6}$$

Where: x is the normalized value of index i; x_i is the observed value of index i; and x_{imax} and x_{imin} are the maximum and minimum values of index i, respectively.

All indices were preprocessed using ArcGIS 10.2, uniformly converted to the Gauss-Kruger projection, It was determined that the spatial location of the data and the values of the attributes corresponded to the actual situation and were spatially analysed on the assumption that the spatial relationships between the ecological indicators were stable over the period of the re-study and would not be significantly altered by changes in time. and resampled into 30 m × 30 m raster data to ensure spatial consistency. All indices were categorized into five vulnerability levels: Extremely low vulnerability, low vulnerability, moderate vulnerability, high vulnerability, and extremely high vulnerability, using different classification methods (Table 3). This process resulted in 17 single-index evaluation maps for Pingquan City (Fig. 2).

2.3.2 Calculation of weights

Objective weights were calculated using the PCA model (Li et al. 2006). This was accomplished using ArcGIS 10.2. To ensure that each principal component contained all relevant indices, the weights of the factors contained in each index were calculated separately. The number of principal components for sensitivity was set to nine, while the number of principal components for resilience and pressure was set to four. The contribution rates and cumulative contribution rates of each principal component were calculated, and principal components with cumulative contribution rates exceeding 85% were selected for ecological vulnerability assessment (Table 4). Equation (7) was used to calculate the weight of each index (w_{lj}):

Table 2 Soil N, P, K composite nutrient index division

Indicator	K_i	100	90	70	50	30
N	(g/kg)	>2	>1.5–2	>1–1.5	>0.75–1	≤0.75
P		>1	>0.8–1	>0.6–0.8	>0.4–0.6	≤0.4
K		>25	>20–25	>15–20	>10–15	≤10

Table 3 Grading criteria for ecological vulnerability assessment in Pingquan City

| Factor	Indicator	Very low vulnerability	Low vulnerability	Moderate vulnerability	High vulnerability	Very high vulnerability	Grading standard
Ecological sensitivity	X1	Quaternary terrestrial loose accumulation formation	Jurassic-Cretaceous medium-acidic ejecta formation; Precambrian medium-acidic rock formation	Precambrian basement rock formation; Precambrian regional metamorphic rock formation; Precambrian contact metamorphic rock formation	Triassic-Cretaceous terrestrial clastic formation; Jurassic-Cretaceous volcanic clastic formation; Sinian-Permian sandy clastic formation; Sinian-Carboniferous argillaceous clastic formation	Sinian-Permian marine carbonate rock formation	Field survey validation
	X2 (°)	<2	[2,6)	[6,15)	[15,25)	≥25	TD/T1055-2019
	X3 (m)	<595	[595,741)	[741,909)	[909,1152)	≥1152	Natural breakpoint method
	X4 (mm)	>582	(528,582]	(478,528]	(432,478]	≤432	Natural breakpoint method
	X5 (°C)	>9.2	(8.6,9.2]	(7.8,8.6]	(6.5,7.8]	≤6.5	Natural breakpoint method
	X6	>30.7	(28.2,30.7]	(26.1,28.2]	(23.3,26.1]	≤23.3	Natural breakpoint method
	X7	>0.91	(0.72,0.91]	(0.49,0.72]	(0.18,0.49)	≤0.18	Natural breakpoint method
	X8	<0.03052	[0.03052,0.03068)	[0.03068,0.03085)	[0.03085,0.03110)	≥0.03110	Natural breakpoint method
	X9	<23.28	[23.28,48.46)	[48.46,82.89)	[82.89,164.67)	≥164.67	Natural breakpoint method
Ecological resilience	X10	>557.6	(486.8,557.6]	(430.4,486.8]	(214.2,430.4]	≤214.2	Natural breakpoint method
	X11		Brown soil	Cinnamon soil	Damp soil	Coarse aggregate soil	Field survey validation
	X12	(96.6,100]	(91.8,96.6]	(87.3,91.8]	(80,87.3]	<80	Natural breakpoint method
	X13	>86.55	(76.66,86.55]	(68.63,76.66]	(53.13,68.63]	≤53.13	Natural breakpoint method
Ecological pressure	X14 (persons/km²)	<83	[83,124)	[124,141)	[141,169)	≥169	Natural breakpoint method
	X15 (million/km²)	<336	[336,374)	[374,444)	[444,727)	≥727	Natural breakpoint method
	X16/t	<1283	[1283,8022)	[8022,12963)	[12963,19230)	≥19230	Natural breakpoint method
	X17/million	<9326	[9326,19168)	[19168,28566)	[28566,38376)	≥38376	Natural breakpoint method
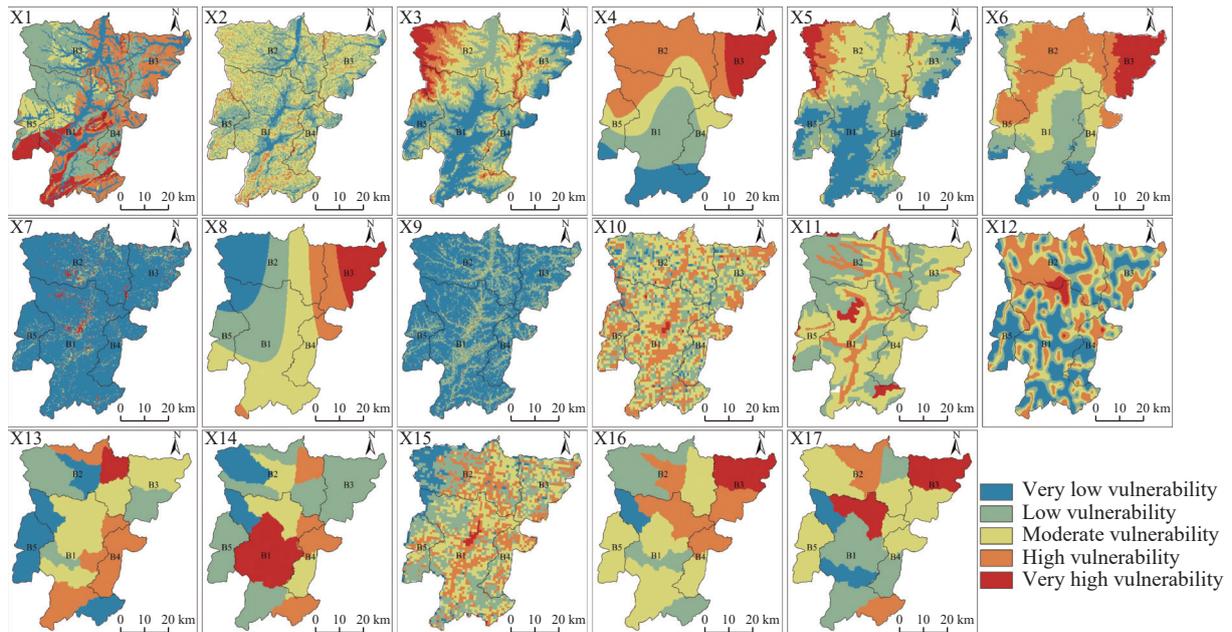
Fig. 2 Single-indicator evaluation map of ecological-geological vulnerability in Pingquan City

Table 4 The load of each index factor in the study area

Typology	F1	F2	F3	Typology	F1	F2	F3	Typology	F1	F2	F3
Sensitivity	−0.070	−0.027	0.997	Resilience	0.926	0.369	0.075	Pressure	−0.370	0.929	−0.001
X1	0.846	−0.453	−0.014	X10	0.045	−0.011	−0.043	X14	−0.024	0.983	−0.167
X2	0.111	−0.093	−0.213	X11	0.988	−0.147	0.009	X15	0.015	0.089	0.071
X3	−0.081	−0.174	−0.459	X12	−0.007	−0.002	0.999	X16	0.653	0.136	0.741
X4	0.406	0.637	0.028	X13	0.147	0.989	0.002	X17	0.757	−0.088	−0.646
X5	0.121	0.155	0.455								
X6	0.278	0.455	−0.214								
X7	0.065	−0.050	−0.136								
X8	0.039	−0.296	0.570								
X9	0.057	−0.169	−0.383								
Eigenvalue	0.073	0.046	0.035	Eigenvalue	0.118	0.036	0.012	Eigenvalue	0.064	0.031	0.006
Variance/%	36.13	22.663	17.52	Variance/%	69.45	21.169	7.027	Variance/%	61.343	30.180	5.790

$$H_j = \sum_{j=1}^{m} \lambda_{jk}^2 (j = 1,2,3,\cdots m,\ \ k = 1,2,3\cdots)$$

$$W_{1j} = H_j / \sum_{j=1}^{n} H_j (j = 1,2,3,\cdots n) \tag{7}$$

Where: H_j is the variance of each factor; W_{1j} is the weight of each principal component; j is the number of indices; k is the number of remaining principal components; and λ_{jk} is the eigenvector of index j on principal component k.

Subjective weights were determined using the AHP model, establishment of Ranking Matrix of Ecological Vulnerability Indicators in Pingquan City (Tables 5, 6 and 7), and the consistency of the judgment matrix was assessed by calculating the Consistency Ratio (CR) using Equation (8). When

the CR value is less than 0.1, the judgment matrix is considered to have acceptable consistency:

$$CR = \frac{CI}{RT} = \frac{\lambda_{max} - n}{RI(n-1)} \tag{8}$$

Where: CR is the consistency index; RI is the random consistency index; λ_{max} is the largest eigenvalue of the judgment matrix; and n is the number of indices. In this study, the CR value was 0.051, indicating reasonable consistency.

The entropy weighting model was established by combining the AHP and PCA, resulting in the comprehensive weights for each index. To mitigate the uncertainty in determining subjective weights (W_{2j}) and objective weights (W_{1j}), the minimum information entropy theory was used to

Table 5 Judgement matrix for evaluation of ecological sensitivity indicators in Pingquan City

Typology	X1	X2	X3	X4	X5	X6	X7	X8	X9
X1	1								
X2	1/8	1							
X3	1/8	1	1						
X4	1/8	1/4	1/4	1					
X5	1/8	1/2	1/2	1/2	1				
X6	1/9	1/2	1/3	1	1	1			
X7	1/2	1	1/2	1/2	1/4	1/3	1		
X8	1	1/6	1/6	1/6	1/6	1/6	1/6	1	
X9	1/2	1/2	1/6	1/8	1/8	1/6	1/4	1/8	1

Table 6 Judgement matrix for evaluation of ecological resilience indicators in Pingquan City

Typology	X10	X11	X12	X13
X10	1			
X11	1/4	1		
X12	1/2	1/2	1	
X13	1	1/4	1/2	1

Table 7 Judgement matrix for evaluation of ecological pressure indicators in Pingquan City

Typology	X14	X15	X16	X17
X14	1			
X15	1	1		
X16	1/4	1/2	1	
X17	1/4	1/2	1/6	1

compute the combined weight (W_j). The closer W_j is to W_{1j} and W_{2j}, the more accurate the weights. The comprehensive weights of the indices (Table 8) were calculated using Equation (9):

$$W_j = \frac{(w_{1j}w_{2j})^{0.5}}{\sum\limits_{j=1}^{m}(w_{1j}w_{2j})^{0.5}}(j=1,2,3,\cdots m) \qquad (9)$$

2.3.3 Comprehensive evaluation of the EVI index
According to the PCA-AHP entropy weighting model, the Ecological Vulnerability Index (EVI) was calculated as the sum of weighted indices. The final *EVI* value was obtained using Equation (10):

$$EVI = \sum_{i=1}^{n} W_i \times X_i \qquad (10)$$

Where: *EVI* is the composite EVI; W_i is the combined weight of index *i*; and X_i is the normalized value of index *i*. The *EVI* ranges from 0 to 1; a higher *EVI* indicates a more vulnerable ecosystem.

To thoroughly analyze ecological vulnerability trends and the overall ecosystem condition, the *EVI* was classified into five levels: I (very low vulnerability), II (low vulnerability), III (medium vulnerability), IV (high vulnerability), and V (very high vulnerability), using the natural break classification method in ArcGIS 10.2.

Table 8 Weights of ecological vulnerability evaluation indicators in Pingquan City (w_j is the comprehensive weight; w_{1j} is the weight calculated by PCA; w_{2j} is the weight obtained by AHP)

Typology	W_{1j}	W_{2j}	W_j	Typology	W_{1j}	W_{2j}	W_j
Ecological sensitivity	0.197	0.655	0.416	Ecological resilience	0.690	0.211	0.442
Geo-construction (X1)	0.1	0.349	0.216	Vegetation NPP (X10)	0.098	0.387	0.21
Elevation (X2)	0.051	0.101	0.083	Soil type (X11)	0.425	0.282	0.373
Altitude (X3)	0.001	0.125	0.013	Soil nutrient synthesis (X12)	0.15	0.175	0.174
Annual rainfall (X4)	0.215	0.086	0.157	Ecological richness (X13)	0.327	0.156	0.243
Average annual temperature (X5)	0.152	0.095	0.139	Ecological pressure	0.113	0.134	0.142
Dryness index (X6)	0.157	0.085	0.134	Population density (X14)	0.252	0.4	0.335
Vegetation cover (X7)	0.08	0.07	0.087	GDP (X15)	0.13	0.291	0.205
Soil erosion factor (X8)	0.163	0.061	0.115	Food crop production (X16)	0.405	0.217	0.313
Landscape fragmentation (X9)	0.081	0.028	0.055	Gross output value of agriculture, forestry, livestock and fisheries (X17)	0.213	0.092	0.148

2.3.4 Geodetectors

The geodetectors employed in this study were developed based on the statistical method for detecting spatial variability proposed by Wang Jinfeng et al (Zhao et al. 2021). Through the analysis of spatial variation patterns of geographic elements, the root factors driving spatial variability were explored. This approach aids in identifying and analyzing the main factors influencing ecological vulnerability and their mechanisms of action. Two analytical methods were used to analyze the ecological vulnerability of Pingquan City: The factor detector, which reveals spatial distribution differences in vulnerability and the explanatory power of each factor, and the interaction detector, which investigates the pairwise interactions between influencing factors and their combined effects on ecological vulnerability.

3 Results and discussion

3.1 Characteristics of EVI spatial distribution

The distribution of ecological sensitivity, resilience, pressure, and the overall EVI in Pingquan City was analyzed using Equation (10) and the weighted overlay function of the ArcGIS platform. The results are presented in Fig. 3. The findings indicate that the overall EVI value for Pingquan City was 0.389, reflecting a moderate level of ecological vulnerability in the region. Furthermore, based on the data in Table 9, the distribution of ecological vulnerability levels in Pingquan City showed a predominance of level II (25%), followed by level IV (24%), level III (21%), level I
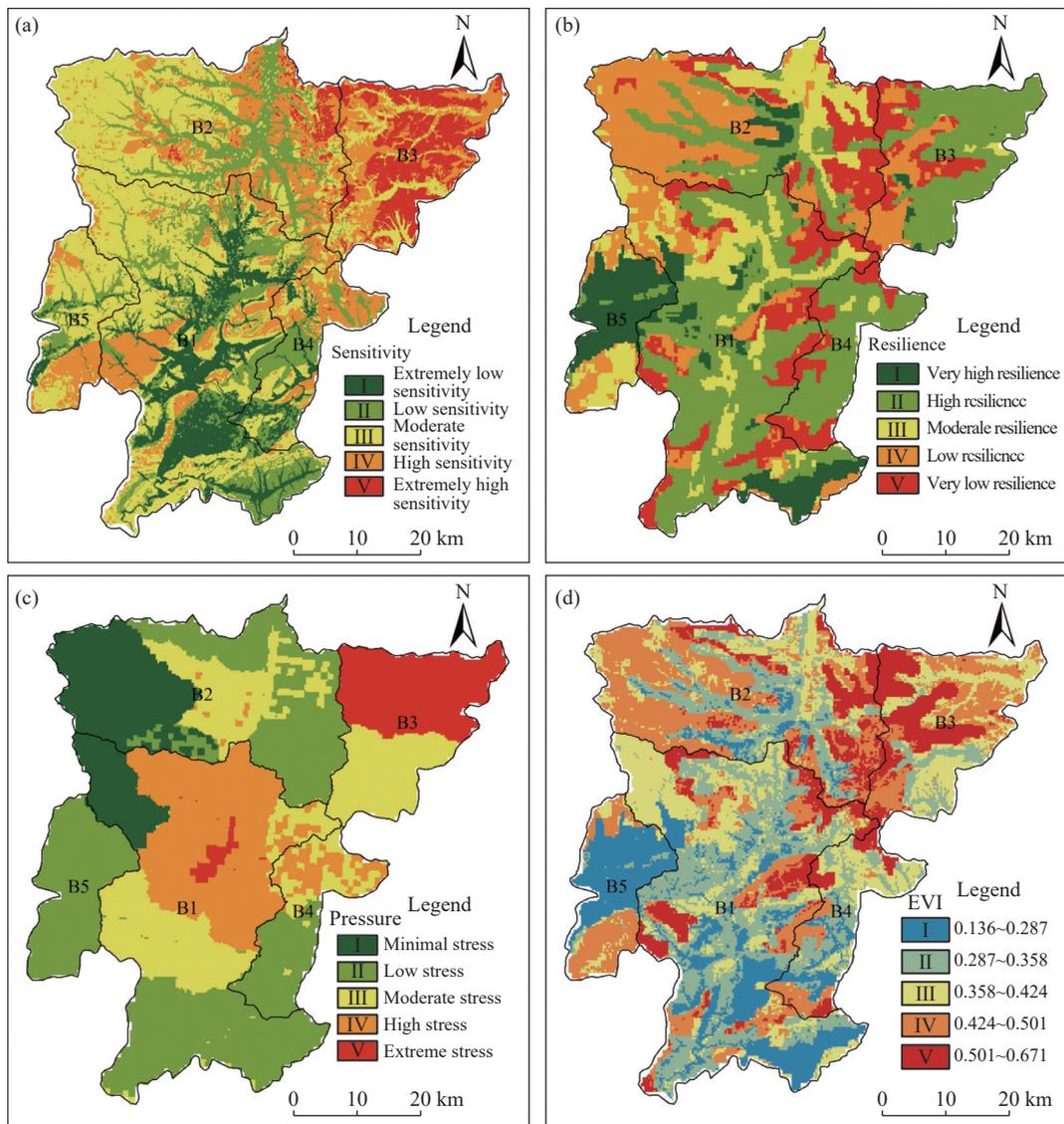

Fig. 3 Ecological vulnerability assessment of Pingquan City (a: Ecological sensitivity assessment; b: Ecological resilience assessment; c: Ecological pressure assessment; d: Ecological Vulnerability Assessment)

(16%), and level V (14%). This suggests that the overall ecological vulnerability of Pingquan City is relatively mild. At the watershed scale, the EVI values exhibited distinct characteristics across different watersheds (Fig. 3a and 4a). Specifically, the EVI values followed the order of B3 watershed (0.459) > B2 watershed (0.416) > B4 watershed (0.380) > B1 watershed (0.361) > B5 watershed (0.321). Watershed B3 was characterized by extremely high sensitivity, with a spatial gradient where sensitivity gradually decreased from northeast to southwest. This pattern indicates that the B3 watershed should be prioritized for ecological restoration efforts. The areas of low resilience were concentrated in the east-central part of the study area and displayed a strip-like distribution. The distribution of ecological pressure by township (Fig. 3c) shows that the northern part of the B3 watershed experienced relatively high ecological pressure due to the intensive development of food crop cultivation and the vegetable, fruit, and forestry industries.

Table 9 Area ratio of different vulnerability classes of EVI in Pingquan City

Typology	I	II	III	IV	V
Area (km^2)	500.91	783.60	680.92	755.50	433.36
Area ratio (%)	16	25	21	24	14

The data in Fig. 4b and Table 10 reveal significant differences in the spatial distribution of ecological vulnerability, sensitivity, resilience, and pressure among the watersheds in the study area (Luo et al. 2024). In terms of ecological vulnerability as indicated by EVI, watershed B3 had the highest proportion of extremely high vulnerability areas, covering 29.63% of its total area. In contrast, watershed B5 had the lowest proportion, with only 0.06% of its area categorized as extremely high

vulnerability. The sensitivity analysis shows that watershed B3 was predominantly composed of areas with high and extremely high sensitivity, accounting for 34.16% and 47.29% of the watershed, respectively. Watershed B2 had a more balanced sensitivity distribution, with an overall moderate sensitivity level. Watersheds B1, B4, and B5, aside from small areas of extremely high sensitivity, exhibited wide variations in sensitivity, reflecting the diverse sensitivity characteristics of watersheds in the hilly region. In terms of resilience, watersheds B2 and B3 had relatively large areas of extremely high resilience, accounting for 40.26% and 34.22% of their respective areas. However, watershed B5 displayed a polarization in resilience, as very low resilience areas and high resilience areas occupied 54.15% and 40.43% of the watershed, respectively. Regarding ecological pressure, watersheds B2 and B5 were subjected to relatively low ecological pressure. In contrast, watershed B3 experienced both moderate and extremely high levels of ecological pressure. Watersheds B1 and B4 showed a broader distribution of pressure levels, covering all levels.

The above analysis suggests that the overall ecological vulnerability of the study area is relatively mild. However, the five watersheds display significant differences in ecological vulnerability: The B3 watershed, which is the Daling River Basin, is characterized by high ecological sensitivity and pressure, with the highest EVI value. This indicates that the region is highly responsive to environmental changes, and human activities are exerting profound impacts on the ecological environment. These activities may not only disrupt the relatively stable structure of the ecosystem but also lead to a series of ecological dysfunctions and degradation. Over time, the B3 watershed, which is currently in a state of moderate vulnerability, could gradually shift toward a high vulnerability state
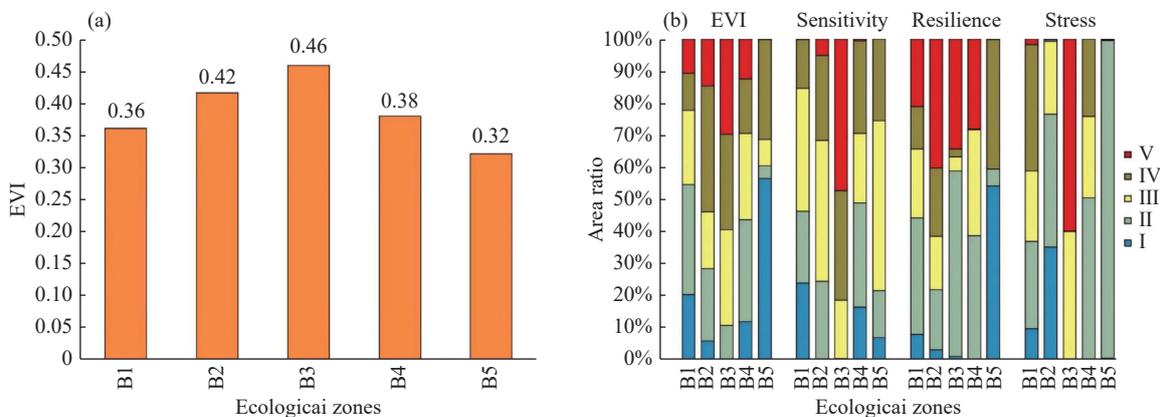

Fig. 4 Mean EVI values (a) and area ratios of EVI to each element (b) for different watershed districts in the Pingquan area

Table 10 Ratio of EVI to area of each element in different watersheds in Pingquan region

Basin	Ecological Vulnerability (%)					Ecological sensitivity (%)				
	I	II	III	IV	V	I	II	III	IV	V
B1	20.29	34.34	23.10	11.55	10.72	23.80	22.42	38.41	15.26	0.11
B2	5.80	22.60	17.68	39.38	14.53	0.01	24.40	43.94	26.58	5.08
B3	0.00	10.71	29.81	29.85	29.63	0.00	0.21	18.34	34.16	47.29
B4	11.80	31.85	26.96	17.04	12.36	16.41	32.46	21.68	28.93	0.53
B5	56.60	3.87	8.21	31.27	0.06	6.80	14.71	53.01	25.49	0.00

Basin	Ecological resilience (%)					Ecological pressure (%)				
	I	II	III	IV	V	I	II	III	IV	V
B1	7.88	36.41	21.43	13.16	21.12	9.64	27.30	21.91	39.40	1.75
B2	3.05	18.79	16.65	21.26	40.26	35.18	41.42	22.70	0.62	0.09
B3	0.97	57.91	4.43	2.46	34.22	0.00	0.18	39.82	0.08	59.92
B4	0.00	38.62	33.13	0.22	28.03	0.00	50.50	25.40	24.10	0.00
B5	54.15	5.29	0.06	40.43	0.07	0.45	99.10	0.19	0.26	0.00

due to increasing anthropogenic disturbances. In contrast, watersheds B1, B4, and B5 generally showcase more favorable ecological conditions, characterized by low sensitivity, high resilience, and relatively low ecological pressure. However, in the northern part of watershed B1, which is the Baohe River Basin and hosts the main urban area, the high intensity of human activities, including extensive mineral extraction, has disrupted the ecological balance. As a result, this part has high ecological vulnerability. This highlights that even in watersheds with generally favorable ecological conditions, high-intensity human activities are a key driver of localized ecological vulnerability. In watershed B2, the ecological indices follow a strip-like distribution along the valley, exhibiting moderate sensitivity, low resilience, and relatively low ecological pressure overall. The alluvial flood-plain at the bottom of the B2 watershed is characterized by fertile soil, abundant water resources, and a suitable climate. Therefore, this area boasts a stable and resilient ecosystem and, consequently, low vulnerability. In contrast, the high-elevation remnant areas of the B2 watershed are characterized by steep slopes, poor soil, and concentrated, unevenly distributed rainfall, leading to significantly higher vulnerability. Thus, the high-altitude mountainous areas of the B2 watershed are typified by high vulnerability.

3.2 Analysis of mechanisms driving spatial variation in ecological vulnerability

Based on the significant spatial variation of ecological vulnerability in the study area, this study employed the EVI as the evaluation metric. Using the K-means classification algorithm, 17 related assessment indices were discretized to analyze the driving mechanisms behind the spatial differentiation of ecological vulnerability. The processed continuous variables were input into the geodetector model as independent variables, and the q-value was selected as a statistic to quantitatively analyze the influence of each factor on the spatial differentiation of EVI.

The results of the factor detector analysis (Table 11) show that the influencing factors of ecological vulnerability in Pingquan City exhibited a certain degree of stability. Among these factors, soil type (X11) had the most significant impact, far surpassing other indices, making it the primary driving factor behind changes in regional ecological vulnerability. Elevation (X3), average annual temperature (X5), and soil erosion (X8) were identified as secondary factors affecting ecological vulnerability. The q-values for the remaining indices were generally low, indicating their relatively limited role in explaining the spatial heterogeneity of ecological vulnerability in Pingquan City.

An interaction detector analysis (Fig. 5) revealed 136 synergistic interactions among the 17 evaluation indices. The strength of these interactions varied widely, with values ranging from a maximum of 0.708 to a minimum of 0.014. Among these interactions, the interaction between ecological abundance (X13) and soil type (X11) was the strongest, indicating a high degree of synergy when both factors jointly influence ecological vulnerability. Furthermore, the interaction effects of soil type (X11) with most other indices were

Table 11 Detection results of factors in Pingquan area

Indicator	q value	Indicator	q Value	Indicator	q Value
Geo-construction (X1)	0.123	Vegetation cover (X7)	0.014	Ecological richness (X13)	0.120
Elevation (X2)	0.083	Soil erosion factor (X8)	0.188	Population density (X14)	0.027
Altitude (X3)	0.248	Landscape fragmentation (X9)	0.084	GDP (X15)	0.051
Annual rainfall (X4)	0.105	Vegetation NPP (X10)	0.025	Food crop production (X16)	0.084
Average annual temperature (X5)	0.220	Soil type (X11)	0.543	Gross output value of agriculture, forestry, livestock and fisheries (X17)	0.070
Dryness index (X6)	0.040	Soil nutrient synthesis (X12)	0.035		

significantly stronger than interactions among other factors, underscoring the central role of soil type in driving changes in ecological vulnerability in Pingquan City. In contrast, the interactions between other factors were relatively weak and did not sufficiently explain the spatial heterogeneity of ecological vulnerability.
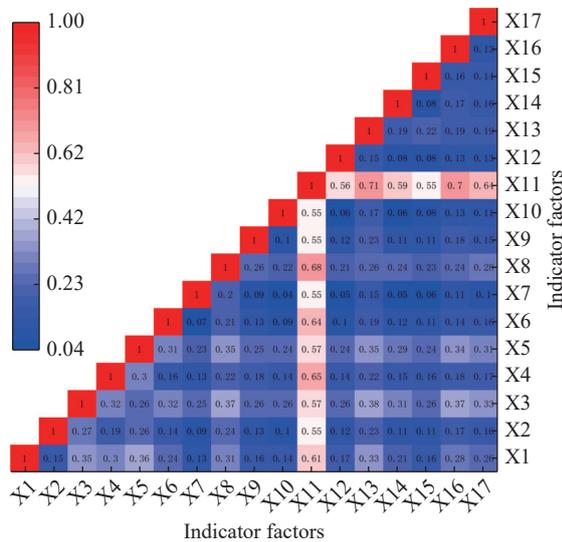
Fig. 5 Interaction detector results for the Pingquan area

In summary, soil type is the key driving factor for ecological vulnerability in Pingquan City, with an influence far exceeding that of any other single index. Meanwhile, elevation, average annual temperature, and soil erosion, as secondary factors, also play a role in shaping ecological vulnerability to some extent. The strong interaction between ecological abundance and soil type further highlights the complex interdependencies among various factors within the ecosystem. Therefore, when formulating strategies for ecological protection and restoration, priority should be given to the conservation and improvement of soil types. In addition, the synergistic effects among different factors must be fully considered to achieve effective management and improvement of ecological vulnerability.

3.3 Exploration of methodological applicability and countermeasures

In this study, 17 evaluation indicators were used to construct an evaluation system based on the SRP model, which is conducive to revealing the vulnerability of the ecological environment from multiple dimensions and levels. Although the accuracy and reliability of the evaluation can be improved, the data sources of too many evaluation indicators may have spatial and temporal differences, affecting the accuracy and reliability of the evaluation results. The use of PCA and AHP to jointly determine the weights of the indicators makes the weight allocation more scientific by using the objective calculation of the mathematical model as well as considering the subjective empirical judgement of the experts. However, different experts may give different judgement matrices and weight allocation results, which may lead to uncertainty in the evaluation results. Although the SRP model has some generality in ecological vulnerability assessment, ecosystems in different regions have unique characteristics and differences. Therefore, when applying the SRP model, appropriate adjustments and modifications should be made according to the actual situation to ensure the accuracy and reliability of the assessment results.

The ecological status of the country's major river basins is a matter of concern, and human activities have exacerbated ecological vulnerability. The Tarim (Xue et al. 2019) and Yinma River basins (Zhang et al. 2017) are seriously disturbed and face ecological challenges. The Yellow River Basin (Zhang et al. 2022) is in trouble due to drought, water shortage and human interference. Pollution loads in the Yellow River Delta (Zhang et al. 2017) have increased a thousand-fold in five years, and wetland ecosystems have been severely damaged. The upper basin of the Enjiang River Basin (Li et al. 2009) is characterised by intensive agricultural activities, water pollution, deforestation and degradation, and ecosystems and biodiversity are being

severely tested. Similar to these watersheds, Pingquan City faces the challenge of ecological vulnerability. As the core area of water conservation in Beijing-Tianjin-Hebei, Pingquan City has the typical characteristics of a small watershed in the hilly area, and its ecological environment has also been strongly affected by human activities. In recent years, due to irrational human activities such as indiscriminate mining, the ecosystem of Pingquan City has become imbalanced, and the problem of ecological vulnerability has become more serious. These problems not only affect the quality of the local ecological environment, but also pose a threat to the water conservation function of the Beijing-Tianjin-Hebei region.

The Daling River Basin, as an area of extremely high sensitivity concentration and with an ecological vulnerability class of IV and V, should be the focus of ecological restoration. Its ecological resilience should be enhanced through measures such as vegetation restoration and soil and water conservation. At the same time, reduce the intensity of human activities in the region, especially the excessive development of agriculture and forestry. The intensive development of food crop cultivation and the vegetable, fruit and forestry industries has resulted in relatively high ecological pressure on the region. Therefore, the industrial layout of these regions should be appropriately adjusted to reduce the pressure of agricultural activities on the ecological environment. The east-central part of the study area needs to focus on soil improvement and vegetation restoration to improve soil fertility and vegetation cover. It is also recommended that mining should be rationally planned in mining areas, green mine construction should be promoted and the development of ecological agriculture and forestry should be encouraged.

Regarding the drivers of ecological vulnerability, soil type was found to be a key driver of ecological vulnerability in the Pingquan area, with an impact far greater than any other single indicator. This finding is consistent with the analyses of the Factor Probe and the Interaction Probe, showing the central role of soil type in changes in ecological vulnerability. Soil type not only affects aspects such as soil fertility, water retention and biodiversity, but also has complex interactions with other ecological factors such as elevation and temperature. Although soil type is the main driver, other factors such as elevation, mean annual air temperature and soil erosion sub are also involved in the process of ecological vulnerability change to some extent. There are complex interactions between these factors and soil types, which

together affect the stability and vulnerability of ecosystems. Therefore, when formulating ecological protection and restoration strategies, the synergistic effects among the factors need to be fully considered in order to achieve effective management and improvement of ecological vulnerability.

4 Conclusion

In this study, an innovative and comprehensive EVI model was developed to account for the unique geographic, climatic, and human characteristics of typical small watersheds in hilly areas of the Beijing-Tianjin-Hebei water conservation zone. The model effectively revealed the overall ecological conditions in Pingquan City. The EVI value of 0.389 suggests a moderate level of ecological vulnerability. However, significant differences were observed between the watersheds. Daling River Basin exhibited the highest EVI value, with ecological vulnerability mainly classified as levels IV and V. Areas of extremely high sensitivity were concentrated in this watershed, which also faced considerable ecological pressure. In contrast, Laoniu River Basin had the lowest EVI value. A high proportion (56.60%) of its area experienced extremely low vulnerability, and the watershed faced very low ecological pressure. These inter-watershed differences highlight the importance of tailoring ecological management strategies to local conditions.

The driving mechanism of spatial variability shows that soil type is the key driving force of ecological vulnerability in Pingquan City. Its influence far exceeds that of other indices. Elevation, average annual temperature, and soil erosion are secondary factors that also play a role in shaping ecological vulnerability to some extent. The strong interaction between ecological abundance and soil type reveals the complex relationships among factors within the ecosystem. When formulating strategies for ecological protection and restoration, emphasis should be placed on the protection and improvement of soil types. In addition, the synergistic effects among various factors should be fully considered to achieve effective management and improvement of ecological vulnerability.

The management of ecological vulnerability in Pingquan City should be guided by its spatial distribution patterns and autocorrelation characteristics. Priority should be given to key regions and core driving factors to rapidly restore fragile ecosystems through targeted and efficient measures. At the same time, comprehensive moni-

toring and assessment across the entire region should be maintained to ensure the thoroughness and sustainability of ecological management efforts.

Acknowledgement

References

Cui C. 2012. The study of ecological environment evolution and countermeasures in source area of the Three Rivers. In Proceedings of the 5th International Yellow River Forum on Ensuring Water Right of the River's Demand and Healthy River Basin maintenance, Minist Water Resources, Yellow River Conservancy Commiss, Zhengzhou, China, 24–28 September.

De Lange HJ, Sala S, Vighi M, et al. 2010. Ecological vulnerability in risk assessment—A review and perspectives. Science of the Total Environment, 408(18): 3871−3879. DOI: 10. 1016/j.scitotenv.2009.11.009.

Fan ZW, Liu MS, Shen WQ, et al. 2009. GIS-based assessment on eco-vulnerability of Jiangxi Province. In 2009 International Conference on Environmental Science and Information Application Technology (Vol. 3, pp. 426–431). IEEE. DOI: 10.1109/ESIAT. 2009.321.

Gao Y, Zhang H. 2018. The study of ecological environment fragility based on remote sensing and GIS. Journal of the Indian Society of Remote Sensing, 46, 793–799. DOI: 10.1007 /s12524-018-0759-1.

Hou K, Li X, Wang J, et al. 2016. Evaluating ecological vulnerability using the GIS and Analytic Hierarchy Process (AHP) Method in Yan'an, China. Polish Journal of Environmen-

tal Studies, 25(2). DOI:10.15244/pjoes/61312.

Hou K, Li X, Zhang J. 2015. GIS analysis of changes in ecological vulnerability using a SPCA model in the Loess plateau of Northern Shaanxi, China. International Journal of Environmental Research and Public Health, 12(4): 4292−4305. DOI: 10.3390/ ijerph120404292.

Hu X, Ma C, Huang P, et al. 2021. Ecological vulnerability assessment based on AHP-PSR method and analysis of its single parameter sensitivity and spatial autocorrelation for ecological protection–A case of Weifang City, China. Ecological Indicators, 125: 107464. DOI: 10.1016/j.ecolind.2021.107464.

Ippolito A, Sala S, Faber JH, et al. 2010. Ecological vulnerability analysis: A river basin case study. The Science of the Total Environment 408 (18): 3880–3890. DOI: 10.1016/j. scitotenv.2009.10.002.

Jiang W, Deng L, Chen L, et al. 2009. Risk assessment and validation of flood disaster based on fuzzy mathematics. Progress in Natural Science, 19(10): 1419−1425. DOI: 10.1016/j. pnsc.2008.12.010.

Lan G, Jiang X, Xu D, et al. 2023. Ecological vulnerability assessment based on remote sensing ecological index (RSEI): A case of Zhongxian County, Chongqing. Frontiers in Environmental Science, 10: 1074376. DOI: 10.3389/fenvs.2022.1074376.

Leitao AB, Ahern J, 2002. Applying landscape ecological concepts and metrics in sustainable landscape planning. Landscape and Urban Planning, 59(2): 65–93. DOI: 10.1016 /S0169-2046(02)00005-1.

Li A, Wang A, Liang S, et al. 2006. Eco-environmental vulnerability evaluation in mountainous region using remote sensing and GIS—A case study in the upper reaches of Minjiang River, China. Ecological Modelling, 192(1-2): 175−187. DOI: 10.1016/j.ecolmodel.2005.07. 005.

Li AN, Wang AS, He XR, et al. 2006. Integrated evaluation model for eco-environmental quality in mountainous region Based on Remote Sensing and GIS. Wuhan University Journal of Natural Sciences, 11(4): 969−976. DOI: 10.1007/BF02830196.

Li L, Shi ZH, Yin W, et al. 2009. A fuzzy analytic

hierarchy process (FAHP) approach to eco-environmental vulnerability assessment for the danjiangkou reservoir area, China. Ecological Modelling, 220(23): 3439−3447. DOI：10.1016/j.ecolmodel.2009.09.005.

Li Y, Huang S, 2015. Landscape ecological risk responses to land use change in the Luanhe River Basin, China. Sustainability, 7(12): 16631−16652. DOI：10.3390/su71215835.

Liu JY, Nie HF, Xu L, et al. 2025. Assessment of ecological geological vulnerability in Mu Us Sandy Land based on GIS and suggestions of ecological protection and restoration. China Geology, 8(1): 117−140. DOI：10.31035/cg20230027.

Luo M, Jia X, Zhao Y, et al. 2024. Ecological vulnerability assessment and its driving force based on ecological zoning in the Loess Plateau, China. Ecological Indicators, 159: 111658. DOI：10.1016/j.ecolind.2024.111658.

Qiu PH, Xu XJ, Xie GZ, et al. 2007. Analysis of the ecological vulnerability of the western Hainan Island based on its landscape pattern and ecosystem sensitivity. Acta Ecologica Sinica, 27(4): 1257−1264. DOI：10.1016/S1872-2032(07)60026-2.

Sahoo S, Dhar A, Kar A. 2016. Environmental vulnerability assessment using Grey Analytic Hierarchy Process based model. Environmental Impact Assessment Review, 56: 145−154. DOI：10.1016/j.eiar.2015.10.002.

Shan C, Dong Z, Lu D, et al. 2021. Study on river health assessment based on a fuzzy matter-element extension model. Ecological Indicators, 127: 107742. DOI：10.1016/j.ecolind.2021.107742.

Shi JT, Liu JJ, Zhang JC, et al. 2024. Analysis of soil heavy metal influencing factors and sources in typical small watersheds in shallow mountainous area. Geophysical and Geochemical Exploration, 48(3): 834−846. (in Chinese) DOI：10.11720/wtyht.2024.1270.

Wang XD, Zhang XH, Gao P. 2010. A GIS-based decision support system for regional eco-security assessment and its application on the Tibetan Plateau. Journal of Environmental Management, 91(10): 1981−1990. DOI：10.1016/j.jenvman.2010.05.006.

Wang Z, Su Y. 2002. Analysis of Eco-environment vulnerability characteristics of Hanzhong City, near the water source midway along the route of the south-to-north water transfer project, China. Acta Ecologica Sinica, 38(02): 432−442. DOI：10.5846/stxb201609261944.

Wu C, Liu G, Huang C, et al. 2018. Ecological vulnerability assessment based on fuzzy analytical method and analytic hierarchy process in Yellow River Delta. International Journal of Environmental Research and Public Health, 15(5): 855. DOI：10.3390/ijerph15050855.

Xu W, Dong Z, Li D, et al. 2017. River health evaluation based on the Fuzzy matter-element extension assessment model. Polish Journal of Environmental Studies, 26(3). DOI：10.15244/pjoes/67369.

Xu X, Yang H, Yang D, et al. 2013. Assessing the impacts of climate variability and human activities on annual runoff in the Luan River basin, China. Hydrology Research, 44(5): 940−952. DOI：10.2166/nh.2013.144.

Xue LQ, Wang J, Zhang L, et al. 2019. Spatiotemporal analysis of ecological vulnerability and management in the Tarim River Basin, China. Science of the Total Environment, 649: 876−888. DOI：10.1016/j.scitotenv.2018.08.321.

Yang L, Cheng YP, Wen XR, et al. 2024. Development, hotspots and trend directions of groundwater numerical simulation: A bibliometric and visualization analysis. Journal of Groundwater Science and Engineering, 12(4): 411−427. DOI：10.26599/JGSE.2024.9280031.

Zhang F, Liu X, Zhang J, et al. 2017. Ecological vulnerability assessment based on multi-sources data and SD model in Yinma River Basin, China. Ecological Modelling, 349: 41−50. DOI：10.1016/j.ecolmodel.2017.01.016.

Zhang H, Lin X, Yu G, et al. 2009. Ecological vulnerability assessment in the middle and lower reaches of the Hanjiang river basin. In 2009 3rd International Conference on Bioinformatics and Biomedical Engineering: 1-4. DOI：10.1109/ICBBE.2009.5162677.

Zhang XL, Yu WB, Cai HS, et al. 2018. Review of

the evaluation methods of regional eco-environmental vulnerability. Acta Ecologica Sinica, 38: 5970−5981. DOI：10.5846/stxb201708211502.

Zhang XQ, Wang LK, Fu XS, et al. 2017. Ecological vulnerability assessment based on PSSR in Yellow River Delta. Journal of Cleaner Production, 167: 1106−1111. DOI：10.1016/j.jclepro.2017.04.106.

Zhang XY, Liu K, Wang S, et al. 2022. Spatiotemporal evolution of ecological vulnerability in the Yellow River Basin under ecological restoration initiatives. Ecological Indicators, 135: 108586. DOI：10.1016/j.ecolind.2022.108586.

Zhao Y, Liu L, Kang S, et al. 2021. Quantitative analysis of factors influencing spatial distribution of soil erosion based on geo-detector model under diverse geomorphological types. Land, 10(6): 604. DOI：10.3390/land10060604.

Zou T, Yoshino K, 2017. Environmental vulnerability evaluation using a spatial principal components approach in the Daxing'anling region, China. Ecological Indicators, 78, 405–415. DOI：10.1016/j.ecolind.2017.03.039.

Zou T, Chang Y, Chen P, et al. 2021. Spatial-temporal variations of ecological vulnerability in Jilin Province (China), 2000 to 2018. Ecological Indicators, 133: 108429. DOI：10.1016/j.ecolind.2021.108429.